Proceedings of the 35th European Safety and Reliability & the 33rd Society for Risk Analysis Europe Conference
Edited by Eirik Bjorheim Abrahamsen, Terje Aven, Frederic Bouder, Roger Flage, Marja Ylönen

doi: 10.3850/978-981-94-3281-3_ESREL-SRA-E2025-P8028-cd

Holistic Simulation Model of the Temporal Degradation of Rolling Bearings

Fabian Mauthe, Simon Hagmeyer, and Peter Zeiler

Institute for Technical Reliability and Prognostics (IZP), Esslingen University of Applied Sciences, Germany.
E-mail: fabian.mauthe@hs-esslingen.de, simon.hagmeyer@hs-esslingen.de, peter.zeiler@hs-esslingen.de

Data-driven diagnostic and prognostic methods for engineering systems, especially those employing machine learning, have gained prominence due to their reliance on data rather than physical system understanding. However, industrial applications often face challenges like unbalanced data distributions or limited data availability, as acquiring data is costly and time-intensive. Although some synthetic data sets and simulation models are publicly available, they often do not represent industry-relevant scenarios. Therefore, this work introduces a simulation model for generating representative run-to-failure data, focusing on rolling bearings. The model comprises three modules: the first determines the bearing life and fault type; the second simulates the degradation progression up to the point of failure; the third generates vibration signals reflecting operating conditions and bearing degradation. Each module is designed as a random process and reproduces the inherent variation of, for example, the life under a given load. As a novelty, the model simulates the vibration signals over the entire life of bearings. Furthermore, it is publicly available and can be used to generate arbitrary data. An initial data set is also published and publicly available.

Keywords: PHM, prognostics and health management, degradation simulation, rolling bearing, vibration signal, run-to-failure data, degradation progression.

1. Introduction

Data-driven diagnostic and prognostic methods in Prognostics and Health Management (PHM), particularly those involving machine learning, have gained prominence. These approaches focus on using data rather than relying on an understanding of the system's physical characteristics and degradation processes. However, due to the high costs and time associated with data acquisition, industrial applications are often confronted with scenarios of insufficient data. In particular, this relates to run-to-failure data, as data are required throughout the life of an engineering system (ES). This not only leads to limitations in industrial applications but also affects research and the development of data-driven diagnostic and prognostic methods (Fink et al., 2020).

The generation of synthetic data using simulations of degradation processes represents a potential solution to this problem. In the research community of PHM, such synthetic data sets and, in some cases, even the simulation model itself have been published. However, these data sets and simulation models do not represent the various data scenarios that can occur in industrial applications, for instance, highly imbalanced data distribution or censored data sets (Hagmeyer et al., 2021). The most frequently used synthetic data sets in the context of PHM, which include simulated sensor signals, are run-to-failure data sets of aircraft engines from Saxena et al. (2008) and Arias Chao et al. (2021), generated with the Commercial Modular Aero-Propulsion System Simulation (CMAPSS) model. Both data sets and the simulation model are highly focused on the aircraft engines. They are not suitable for reproducing arbitrary data scenarios. This also applies to other synthetic data sets with their underlying models listed in Mauthe et al. (2024).

Therefore, the objective of this work is to propose a simulation model that enables its users to generate data sets that reflect the data scenarios under investigation. This is achieved by a holistic modeling approach, ranging from the life distribution through the progression of degradation up to the resulting measurement signal, which is used for diagnosis and prognosis. The model deals with a key machine element in the context of PHM—the rolling bearing (Wang et al., 2020). Despite being frequently considered at PHM, the literature on its simulation for data generation is scarce. D'Elia et al. (2018) focus solely on simulating the vibration signal for discrete degradation levels. Hosseinli et al. (2024) and Ai et al. (2023) consider the temporal degradation trend but focus on replicating existing experimental data without a holistic modeling approach. As a result, the proposed model is a novelty in this context, with its holistic approach and the simulation of vibration signals over the entire life of bearings.

An executable application of the simulation model[a] and an initial data set[b] from this model are publicly available. The data set reflects a data scenario in which the lives and degradation progressions vary greatly despite similar operating conditions and the same bearing type. In the following, the novel simulation model is introduced and a data set generated with it. Thereby, Section 2 explains the structure of the model and its functionality. Section 3 presents the life and fault modeling. Section 4 deals with the simulation of degradation progression. The generation of vibration signals constitutes Section 5. Section 6 summarizes the results of this work.

2. Model Structure and Functionality

The main purpose of the model is to support the development of data-driven diagnostic and prognostic methods by giving its users the opportunity to simulate a wide variety of data scenarios. A modular design is selected in order to be able to separately define the life load distribution, the degradation progression, as well as the resulting measurement signals (vibration). These three aspects of the failure characteristics each make up separate modules. The structure of the model is illustrated in Fig. 1 and the functionality is described in the following.

User: The user's input information serves as a foundation. It includes bearing parameters (BP), operating conditions (OC), and simulation details (SD). BP involve all the necessary characteristics and parameters of the rolling bearings to be simulated. The OC contain the parameters under which the bearings are operated. These are parameters that would also have to be defined when generating experimental data. The SD are parameters that are specifically required for the simulation. The input information and the respective parameters are aggregated in tabular form as shown in Fig. 1. There, the i-th row corresponds to the simulation of the i-th bearing.

Module 1: It comprises the life and fault modeling. Here, to generate the run-to-failure data of the bearings, first the load level is drawn from a load distribution function. Based on the load that the bearings experience, a life is determined from a probabilistic life-load model. In addition, the resulting fault type is selected, whereby the load influences the preference of the individual fault type.

Module 2: The determined life is an input for the second module. This simulates how the degradation progresses from the initial state of the bearing up to the specified failure time. The user has various functions at his disposal, each modeling different types of degradation progressions. These functions can include random processes so that, despite the identical life of two bearings, different degradation progressions result.

Module 3: The third module generates vibration measurements for the simulated bearings. They depend on the results of the first two modules with the fault type occurring in the bearing and the degradation progression. Vibration measurement series are calculated equally spaced throughout the life. In this module there are also random effects, such as simulated measurement noise.

The modular structure results in a fanning out of the data volume for each bearing across the modules. While one life is determined in the first module, a progression of degradation values up to this life is determined in the second, and a vibration measurement series for each degradation value is determined in the third. Each module contains random processes that reflect the resulting aleatory uncertainty occurring in realistic applications. The ability to generate any amount of data

[a]Simulation model: https://github.com/PHM-Hochschule-Esslingen/Bearing_Simulation_Model
[b]Data set *Bearings with Varying Degradation Behaviors*: https://www.kaggle.com/datasets/prognosticshse/bearings-with-varying-degradation-behaviors

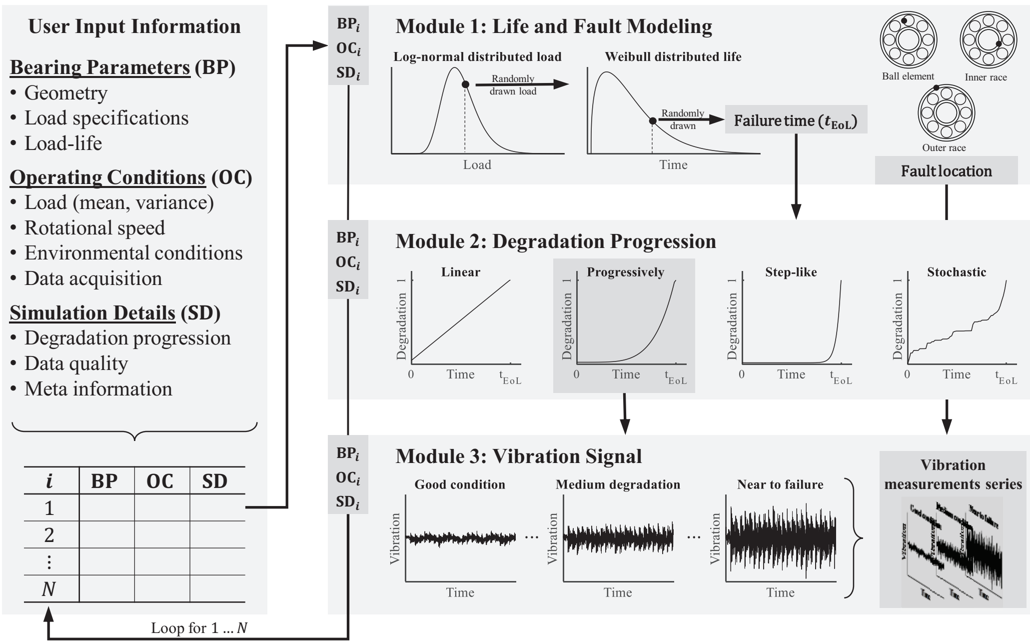

Fig. 1. Visualization of the structure and functionality of the simulation model, exemplarily for one bearing.

with the model allows epistemic uncertainty to be mapped. Hence, the model and its resulting data can also be used for uncertainty considerations. The simulation model is publicly available, where a detailed description of the utilization of the simulation model is provided[c].

3. Life and Fault Modeling

The first module deals with life and fault modeling. For this, Section 3.1 covers the load and Section 3.2 the life determination. Subsequently, Section 3.3 describes the assignment of a fault type. Section 3.4 presents the data generated with the first module for the initial data set.

3.1. *Load*

Often the load experienced in testing or in the field varies. To take this variation and resulting uncertainty into account, the load is modeled as a random variable L with a log-normal distribution. One load level for each bearing is randomly selected based on the corresponding log-normal distribution.

A log-normal distribution is specified by μ and σ^2, resulting in $\mathrm{E}[L] = e^{\mu+\frac{\sigma^2}{2}}$ and $\mathrm{Var}[L] = e^{2\mu+\sigma^2}\left(e^{\sigma^2}-1\right)$. The values of $\mathrm{E}[L]$ and $\mathrm{Var}[L]$ serve as input information for the simulation model and must be defined by the user. Thereby, a user can select a purely deterministic load level by setting $\mathrm{Var}[L] = 0$.

3.2. *Life*

The next step is to determine the life, which depends on the selected load level. The life of rolling bearings can be modeled with a three-parameter Weibull distribution (Bertsche, 2008). The respective probability density function is

$$f(t) = \frac{b}{\eta - t_0} \cdot \left(\frac{t-t_0}{\eta-t_0}\right)^{b-1} \cdot e^{-\left(\frac{t-t_0}{\eta-t_0}\right)^b}. \quad (1)$$

The shape parameter b depends on the design of the rolling element. For ball bearings, $b_{\mathrm{ball}} = 1.1$ applies, and for roller bearings, $b_{\mathrm{roller}} = 1.35$. As these values are based on extensive tests compared to other machine elements, the result is a high

[c]Simulation model: https://github.com/PHM-Hochschule-Esslingen/Bearing_Simulation_Model

statistical confidence (Bertsche, 2008). For this reason, the shape parameters are used as deterministic values. In order to determine the failure-free time t_0 and the characteristic life η, the B_{10} life is calculated first. For this, the modified rating life[d]

$$L_{10m} = a_{\text{ISO}} \cdot \left(\frac{C}{P}\right)^p, \tag{2}$$

defined in standard ISO 281:2007 (International Organization for Standardization, 2007), is employed. C is the dynamic load rating (provided by the bearing manufacturer), P is the equivalent dynamic load (here the drawn load level) and the exponent p depends on the type of rolling element ($p_{\text{ball}} = 3$, $p_{\text{roller}} = {}^{10}/_{3}$). The modification factor a_{ISO} incorporates effects on the bearing life, like lubrication, environmental factors, contaminant particles, and mounting. When a bearing is operated in accordance with established guidelines, $a_{\text{ISO}} = 1$ can be applied. The user of the model has the option to specify this factor. Based on Eq. (2) the characteristic life η is calculated as

$$\eta = \frac{B_{10} - t_0}{\sqrt[b]{-\ln 0.9}} + t_0, \tag{3}$$

with $B_{10} = L_{10m}$ and $t_0 = {}^{f_{tB}}/_{B_{10}}$. In this work, f_{tB} is 0.2 in accordance with Bertsche (2008). Based on the distribution specified, the life of each bearing is randomly selected.

3.3. *Fault location*

Rolling bearing faults commonly arise from localized material degradation, such as pitting, spalling, or corrosion of the main bearing components (inner race, outer race, and rolling elements) (Antoni, 2007). Generally, simultaneous damage to multiple components can occur. However, one component typically predominates in causing failure, as observed in real data (Wang et al., 2020). Therefore, in the context of rolling bearings, a distinction is usually made between these three fault types or damage positions.

The load that an ES experiences not only influences its life but also the probability of one type of failure predominating. In the case of ball bearings, for example, the contact geometry of the three components is different and therefore also the stresses resulting from the load. Thus, depending on the load level, the chances of a certain fault type vary. This also applies to the model described here, where the occurrence of a fault type is also subject to a random process. The influence of the selected load level is done via a weighted random selection. In this case, at low loads, faults on the inner and outer races are more likely, whilst the probability of a rolling element fault increases with the load.

3.4. *Load and lives in the data set*

The data set *Bearings with Varying Degradation Behaviors* generated using the simulation model comprises a total of 40 simulated bearings. Thereby, bearing type *NU204-E-XL-TVP2* is considered, with $a_{\text{ISO}} = 1$, $C = 32,000$ N, and $p = {}^{10}/_{3}$. For all bearings, $\text{E}[L] = 4,500$ N and $\sqrt{\text{Var}[L]} = 100$ N are used. The resulting random load levels are shown in Fig. 2a). Bearing lives are sampled based on the load levels drawn and shown in Fig. 2b). This results in a scattering of the life typical for rolling bearings, with a small variance in the load. The respective fault types are not included in this data set in order to hinder the prediction task for this data set.

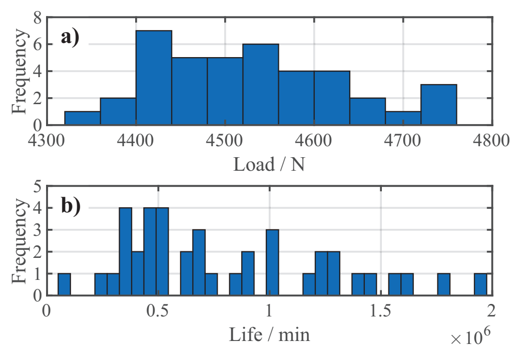

Fig. 2. Load and life samples of the data set. a) randomly drawn load samples using a log-normal distribution. b) random lives of the 40 bearings.

4. Degradation Progression

The aim of the second module is to calculate how degradation progresses from the bearing's new condition to its end of life (EoL). For this purpose,

[d] L_{10m} in 10^6 revolutions, here is converted into minutes

the degradation is defined as a time-dependent function $d(t)$ with the degradation level $d \in [0, 1]$ and time $t \in [0, t_{\mathrm{EoL}}]$. Thereby, $d = 0$ represents a bearing in its new state and $d = 1$ the threshold for the EoL. To model varying production quality, an initial degradation is also defined in the model so that the simulated bearings start with $d(t = 0) = d_0 \geq 0$. Thereby, d_0 is randomly drawn, equally distributed from $[0, 0.05]$. The model provides different types of degradation functions, which can be used for simulating the degradation progression between start and end. As ESs usually lack a form of self-healing, as in the case of rolling bearings, their degradation increases monotonically (Hagmeyer et al., 2022). For this reason, all implemented degradation functions feature such monotonicity.

The following Section 4.1 explains the predefined functions the user can choose for simulating the degradation progression. Thereafter the simulated degradation curves within the data set are presented in Section 4.2.

4.1. *Predefined progression functions*

The degradation progression of an ES often shows a characteristic behavior (Meeker et al., 2022). The model allows the user to choose from several frequently occurring progression functions, whereby the complexity for the resulting diagnostic and prognostic functions differs.

Linear Increasing Degradation: This degradation function connects the random initial degradation $d(0)$ and the determined life $d(t_{\mathrm{EoL}}) = 1$ by a straight line. With this function, the degradation progression of different bearings only varies due to the random-based corner points of the line.

$$d(t) = \frac{1 - d_0}{t_{\mathrm{EoL}}} t + d_0 \tag{4}$$

Progressively Increasing Degradation: In order to simulate a progressively increasing degradation, there exists a variety of mathematical functions. In this case, a power function, as specified by Zhu et al. (2017), is used,

$$d(t) = d_0 + (1 - d_0) \cdot \left(\frac{t}{t_{\mathrm{EoL}}}\right)^a \text{ with } a > 1. \tag{5}$$

The parameter that determines the shape is the exponent a. The higher its value, the more pronounced is the convex course of the degradation. For a typical progressive increase in degradation, a is drawn equally distributed from $[3, 6]$ for each simulated bearing. This additionally increases the variation of the degradation curves and enhances the resemblance to real bearing applications.

Step-like Increasing Degradation: The literature on bearing damage describes that often degradation hardly increases for a long time but increases sharply before failure (Wang et al., 2018). Such a progression can also be simulated by the power function in Eq. (5). For this, however, the value of a is drawn equally distributed from the interval $[15, 35]$.

Randomly Increasing Degradation: The degradation functions described above show a progression that is deterministic for one parameterization. However, the degradation of ESs often shows a stochastic course that includes abrupt rises. To reflect this, the model provides the option to simulate the degradation progression by a gamma process. The gamma process is characterized by independent, non-negative increments. For this reason, it has been used several times for degradation simulation (van Noortwijk, 2009).

The gamma process is sampled through a bridge-sampling. With this sampling method, the final value of the gamma process is sampled first or, in this case, predetermined. The random degradation progression between $t = 0$ and t_{EoL} is then sampled based on conditional probabilities. The essential element here is the beta distribution. For the user, α_γ and β_γ are available as parameters. They scale the inputs for the beta distribution, thus determining the shape of the resulting degradation curve. If both parameters have the same value, the gamma process is stationary with a linear increase in the expected value of the degradation. A convex course of the degradation is achieved by $\alpha_\gamma > \beta_\gamma$ and a concave course by $\alpha_\gamma < \beta_\gamma$. The variance of the gamma process is controlled for a fixed ratio of α_γ and β_γ by their magnitude, whereby small values result in a high variance and thus pronounced stages of degradation. For further information on the gamma process, refer to Avramidis et al. (2003) and van Noortwijk (2009).

4.2. *Degradation curves in the data set*

The published data set serves as an example to illustrate the capabilities of the model. Therefore, each of the four degradation functions described above is used to define the degradation progression of ten bearings. Some of these degradation curves generated are shown in Fig. 3.

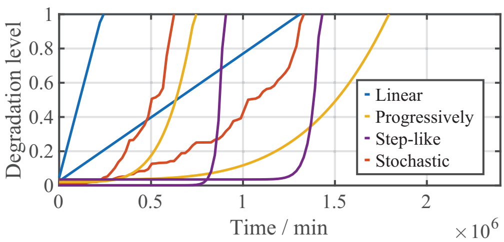

Fig. 3. Examples of degradation curves within the published data set created using the four predefined degradation functions.

5. Vibration Signal

The third module is employed for generating the vibration signal corresponding to the degradation level $d(t)$. The vibrations are primarily caused by the bearing fault. Their modeling is presented in Section 5.1. This is followed by examples of simulated vibration measurements in Section 5.2.

5.1. *Rolling bearing fault model*

When mechanical contact occurs in the bearing that affects the fault location (see Section 3.3), a short impulse, exciting structural resonance within the bearing and its housing, is generated. As the bearing rotates, a series of impulses occurs, with the time between pulses depending on the fault type and the geometry of the bearing. For this, McFadden and Smith (1984) provide a rolling bearing model. The model is extended by Antoni (2007), introducing a ball sliding theory and integrating a random sliding effect, which leads to a rotational model that matches the pulse times of actual bearings more closely. In order to compute the induced impulses, the entire bearing and its supporting structure are compared to a single-degree-of-freedom (SDOF) oscillating system (Hosseinli et al., 2024; Ai et al., 2023). By combining the rotational and impulse models, the vibration signal can be characterized as

$$x(t) = \sum_{i=-\infty}^{+\infty} h(t - iT - \tau_i) q(iT) A_i + n(t). \quad (6)$$

Here $h(\cdot)$ is the impulse response to a single impact, i the index of the i-th impact due to the fault, T the time between two consecutive impacts, and $q(iT)$ the amplitude modulation function of the impulse response due to the load distribution. τ_i accounts for random fluctuations in the interval between two consecutive impacts (i.e., sliding effects). A_i represents random fluctuations in the impulse amplitude. The superimposed signal noise is denoted by $n(t)$. The numerical implementation of D'Elia et al. (2018) is used as a foundation to solve equation Eq. (6). In this work, changes are made to take into account the current level of degradation in order to generate holistic run-to-failure data.

The first step of the vibration simulation is calculating the times at which the fault location is hit based on its angular position. The resulting vector serves as the foundation for the second step, simulating the vibration signal using the SDOF system. In the simulation model, the operating scenario of a rotating inner race and a fixed outer race is considered. Thus, θ corresponds to the current rotational angle of the shaft and inner race. In the model the rotational frequency of the inner

Table 1. Overruns per revolution $n_{\theta_{\text{fault}}}$ for different fault types, where n_r is the number of rolling elements, d the roller diameter, D the pitch circle diameter, and α the contact angle.

Fault	$n_{\theta_{\text{fault}}}$
Outer race	$\frac{1}{2} n_r \left(1 - \frac{d}{D}\cos(\alpha)\right)$
Inner race	$\frac{1}{2} n_r \left(1 + \frac{d}{D}\cos(\alpha)\right)$
Rolling element	$\frac{D}{d}\left(1 - \left(\frac{d}{D}\cos(\alpha)\right)^2\right)$

race $f_r(\theta)$ is implemented to be angle-dependent. Here, the following speed profile is defined to include deviations in the rotational frequency

$$f_r(\theta) = f_{\text{set}} + f_d \cdot \sin(f_m \cdot \theta). \tag{7}$$

f_{set} is the set rotational frequency of the inner race. The deviation is implemented as an angle-dependent frequency shift characterized by f_d and f_m. In addition to the rotational frequency, the angular difference $\Delta\theta_i$ between the overruns of the fault location needs to be calculated. The formulas for the systematic occurrence of overruns per revolution of the shaft $n_{\theta_{\text{fault}}}$ are given in Table 1 for the three fault types. To include a random deviation between two consecutive impacts, $\Delta\theta_{\tau_i}$ is added (corresponding to τ_i in Eq. 6) with $\Delta\theta_{\tau_i} \sim N(\mu_{\theta_{\tau_i}}, \sigma_{\theta_{\tau_i}})$, resulting in

$$\Delta\theta_i = \frac{2\pi}{n_{\theta_{\text{fault}}}} + \Delta\theta_{\tau_i}. \tag{8}$$

Using the speed profile defined in the angular domain and the angular distances, the inter-arrival time between two consecutive impacts can be determined with

$$\Delta T_i = \frac{\Delta\theta_i}{2\pi f_r(\theta_i)}. \tag{9}$$

The SDOF system is excited by an impulse with each impact. Thereby the magnitude of the impulses varies as shown in Eq. (6). For all fault types, variation stems from the random variable A_i. For the inner race and rolling element fault, the variation also results from the function $q(iT)$, which depends on the current angular position and load zone. The impulse response is modeled as

$$h(t) = \frac{J(d(t))}{m\omega_d} e^{-\zeta\omega_n t} \sin(\omega_d t). \tag{10}$$

Here, the level of the respective pulse amplitude depends on the current degradation level $d(t)$. $\zeta = c/2\sqrt{mk}$ is the damping ratio, $\omega_n = \sqrt{k/m}$ is the natural frequency, and $\omega_d = \omega_n\sqrt{1-\zeta^2}$ is the natural damped frequency. In these three equations, m is the mass, k the stiffness, and c the damping coefficient of the SDOF system; all are input parameters by the user. The intended vibration measurement corresponds to the acceleration and therefore the second derivative of Eq. (10).

5.2. *Vibration signals in the data set*

Figure 4 shows examples of simulated vibration measurement series from the published data set for different levels of degradation and the three fault types[e]. It can be seen that an increase in degradation is connected to an increase in the vibration signal magnitude. Moreover, the random amplitude influences are visible, particularly for the outer race fault. Beyond this, the typical amplitude modulation in the signals for the inner race and rolling element fault is also recognizable.

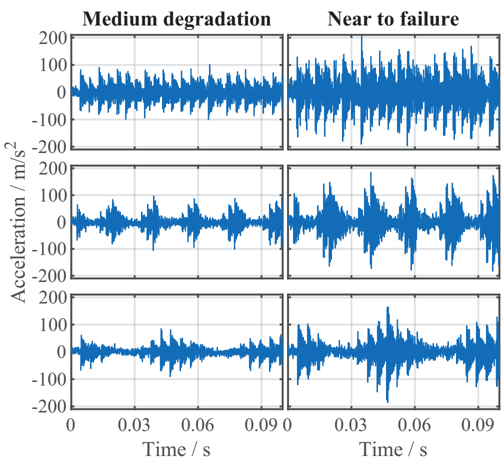

Fig. 4. Vibration signals for an outer race, inner race, and rolling element fault from top to bottom, each with a medium and severe degradation level.

6. Conclusions

Research on data-driven diagnostic and prognostic methods requires convenient access to data that reflect the problem or data scenario being investigated. However, there is a lack of suitable simulation models for flexibly reproducing arbitrary data scenarios. Therefore, this work introduces such a simulation model for the machine element of a rolling bearing. Because the simulation model is intended to be versatile, it is divided into three modules, which allows independent parametrization. These modules consist of the life and fault,

[e] SDOF system with $m = 15,000$ kg, $k = 3.5 \cdot 10^{12}$ N/m, and $c = 10^7$ Ns/m.

the degradation, and the vibration signal modeling. The independent parametrization of these modules provides the user a variety of data scenarios that can be simulated. In addition to this user parametrization, each module is subject to random processes. This allows for controlling epistemic and aleatory uncertainty in diagnosis and prognosis based on the synthetic data of the model. The model presented is being used to generate and publish an initial data set on the run-to-failure of rolling bearings. The model is publicly available and can be used to generate data sets to support research on diagnostic and prognostic methods. In the future, the authors intend to continuously revise the simulation model to incorporate extensions and improvements.

Acknowledgement

The authors wish to acknowledge that the research findings presented in this paper originated in part from the project *TheoMation*, funded by the Deutsche Forschungsgemeinschaft (DFG, German Research Foundation) under grant no. 514247199 and in part from the Program *Professorales Personal an Fachhochschulen (Professorial Staff at Universities of Applied Sciences)*, funded by the German Federal Ministry of Education and Research under grant no. 03FHP115.

References

Ai, T., Z. Liu, J. Zhang, H. Liu, Y. Jin, and M. Zuo (2023). Fully simulated-data-driven transfer-learning method for rolling-bearing-fault diagnosis. *IEEE Transactions on Instrumentation and Measurement 72*, 1–11.

Antoni, J. (2007). Cyclic spectral analysis of rolling-element bearing signals: Facts and fictions. *Journal of Sound and Vibration 304*(3-5), 497–529.

Arias Chao, M., C. Kulkarni, K. Goebel, and O. Fink (2021). Aircraft engine run-to-failure dataset under real flight conditions for prognostics and diagnostics. *Data 6*(1), 5.

Avramidis, A., P. L'ecuyer, and P.-A. Tremblay (2003). Efficient simulation of gamma and variance-gamma processes. In *Proceedings of the 2003 International Conference on Machine Learning and Cybernetics (IEEE Cat. No.03EX693)*. IEEE.

Bertsche, B. (2008). *Reliability in Automotive and Mechanical Engineering*. Berlin, Heidelberg: Springer.

D'Elia, G., M. Cocconcelli, and E. Mucchi (2018). An algorithm for the simulation of faulted bearings in non-stationary conditions. *Meccanica 53*(4-5), 1147–1166.

Fink, O., Q. Wang, M. Svensén, P. Dersin, W.-J. Lee, and M. Ducoffe (2020). Potential, challenges and future directions for deep learning in prognostics and health management applications. *Engineering Applications of Artificial Intelligence 92*, 103678.

Hagmeyer, S., F. Mauthe, and P. Zeiler (2021). Creation of publicly available data sets for prognostics and diagnostics addressing data scenarios relevant to industrial applications. *International Journal of Prognostics and Health Management 12*(2), 1–20.

Hagmeyer, S., P. Zeiler, and M. F. Huber (2022). On the integration of fundamental knowledge about degradation processes into data-driven diagnostics and prognostics using theory-guided data science. *PHM Society European Conference 7*(1), 156–165.

Hosseinli, S. A., T. Ooijevaar, and K. Gryllias (2024). Simulation-based remaining useful life prediction of rolling element bearings under varying operating conditions. *PHM Society European Conference 8*(1), 12.

International Organization for Standardization (2007). Rolling bearings - dynamic load ratings and rating life (iso 281:2007).

Mauthe, F., C. Braun, J. Raible, P. Zeiler, and M. F. Huber (2024). Overview of publicly available degradation data sets for tasks within prognostics and health management. *arXiv* (2403.13694), 1–11.

McFadden, P. D. and J. D. Smith (1984). Model for the vibration produced by a single point defect in a rolling element bearing. *Journal of Sound and Vibration 96*(1), 69–82.

Meeker, W. Q., L. A. Escobar, and F. G. Pascual (2022). *Statistical methods for reliability data* (Second edition ed.). Wiley series in probability and statistics. Hoboken, NJ: Wiley.

Saxena, A., K. Goebel, D. Simon, and N. Eklund (2008). Damage propagation modeling for aircraft engine run-to-failure simulation. In *2008 International Conference on Prognostics and Health Management*, Piscataway, NJ, pp. 1–9. IEEE.

van Noortwijk, J. (2009). A survey of the application of gamma processes in maintenance. *Reliability Engineering & System Safety 94*(1), 2–21.

Wang, B., Y. Lei, N. Li, and N. Li (2020). A hybrid prognostics approach for estimating remaining useful life of rolling element bearings. *IEEE Transactions on Reliability 69*(1), 401–412.

Wang, D., K.-L. Tsui, and Q. Miao (2018). Prognostics and health management: A review of vibration based bearing and gear health indicators. *IEEE Access 6*, 665–676.

Zhu, S.-P., Q. Liu, and H.-Z. Huang (2017). Probabilistic modeling of damage accumulation for fatigue reliability analysis. *Procedia Structural Integrity 4*, 3–10.